Articles

Kinetics of Colloidal Templating Using Emulsion Drop Consolidation

Amy Q. Shen,*,† Danhong Wang,‡ and Patrick T. Spicer‡

Mechanical and Aerospace Engineering, Washington University in St. Louis, St. Louis, Missouri 63130, and Complex Fluids Group, Procter and Gamble Co., West Chester, Ohio 45069

Received May 14, 2007. In Final Form: September 27, 2007

The emulsion templating of ordered colloidal microsphere assemblies by Manoharan et al. involves a consolidation process where dispersed phase fluid is transported from droplets into a continuous phase. Consolidation can be approximated as a diffusion process with moving boundaries. The kinetics of consolidation are investigated here by following droplet shrinkage with time as a prelude to understanding rate effects on assembly structure. Consolidation kinetics are influenced by liquid diffusivity, the number of colloidal particles in a droplet, and the surfactant concentration. While surfactant exhibits little effect well below its critical micelle concentration (CMC) value, it significantly slows consolidation above the CMC. For a specific continuous phase (i.e., silicone oil and fluorinated silicone oil), with proper scalings, the droplet size shrinks with time following a power law independent of droplet diameter, surfactant concentrations, and particle number concentration. The power law exponent varies from 1/2 to 2/3 with different continuous oil phases as a result of concentration and interfacial effects. This study leads to an improved understanding of colloidal microstructure development at interfaces that can be applied in novel materials synthesis and drug delivery areas.

1. Introduction

Colloidal assemblies are promising sources of photonic and encapsulation materials, having received much attention in the past decade. For example, Velev et al. used emulsion droplet templates to form ball-like aggregates of latex particles,[1,2] microstructured hollow spheres[3] and porous particles.[4] Dinsmore et al.[5] fabricated capsules with a wide size range and adjustable permeability via colloidal self-assembly.

Recently, Manoharan et al.[6,7] created symmetric colloidal clusters with 4−15 constituent particles using toluene-in-water emulsions as templates. Toluene is removed from the system via evaporation, shrinking the drops and consolidating the particles to form assemblies. Both oil-in-water and water-in-oil emulsions, as well as various emulsification methods and different colloidal particles, have been used to produce similar clusters.[8−10]

The shrinkage of emulsion droplets with time, referred to as consolidation hereafter, is important for colloidal cluster self-assembly. The dynamics of the consolidation process are of practical interest, as they set the time scale of colloidal assembly. Lauga et al.[11] presented a numerical and theoretical analysis of the mechanism of structure formation during consolidation. In their study a critical volume, below which the droplet cannot remain spherical, is shown to be the determining point in time when packing modification may occur. It is of interest to characterize the consolidation process, as its impact on the final packing of colloidal particles may offer a significant degree of control of structure formation. For example, would the cluster of a given number of spherical particles form the same configuration if the template droplet shrinks at an extremely high rate?

Liquid drops evaporating in air have been widely studied,[12−23] but the dissolution of emulsion droplets in a liquid has received less attention. Clint et al.[24] measured water evaporation in a water-in-dodecane microemulsion system. These studies provide insight in the mechanism and rate-limiting process in the dissolution of emulsion systems. Epstein and Plesset presented a diffusion-based model (EP model) for the dissolution of gas bubble in an infinite solution.[25] This model was further tested

* To whom correspondence should be addressed. E-mail: aqshen@me.wustl.edu.
† Washington University in St. Louis.
‡ Procter and Gamble Co.

(1) Velev, O. D.; Furusawa, K.; Nagayama, K. *Langmuir* **1996**, *12*, 2385.
(2) Velev, O. D.; Nagayama, K. *Langmuir* **1997**, *13*, 1856.
(3) Velev, O. D.; Furusawa, K.; Nagayama, K. *Langmuir* **1996**, *12*, 2374.
(4) Velev, O. D.; Lenhoff, A. M.; Kaler, E. W. *Science* **2000**, *287*, 2240.
(5) Dinsmore, A. D.; Hsu, M. F.; Nikolaides, M. G.; Marquez, M.; Bausch, A. R.; Weitz, D. A. *Science* **2002**, *298*, 1006.
(6) Manoharan, V. N.; Elsesser, M. T.; Pine, D. J. *Science* **2003**, *301*, 483.
(7) Manoharan, V. N.; Pine, D. J. *MRS Bull.* **2004**, 91.
(8) Yi, G.-R.; Manoharan, V. N.; Michel, E.; Elsesser, M. T.; Yang, S.-M.; Pine, D. J. *Adv. Mater.* **2004**, *16*, 1204.
(9) Yi, G.-R.; Thorsen, T.; Manoharan, V. N.; Hwang, M.-J.; Jeon, S.-J.; Pine, D. J.; Quake, S. R.; Yang, S.-M. *Adv. Mater.* **2003**, *15*, 1300.
(10) Cho, Y.-S.; Yi, G.-R.; Kim, S.-H.; Pine, D. J.; Yang, S.-M. *Chem. Mater.* **2005**, *17*, 5006.
(11) Lauga, E.; Brenner, M. P. *Phys. Rev. Lett.* **2004**, *93*, 238301.
(12) Anderson, D. M.; Davis, S. H. *Phys. Fluids* **1995**, *7*, 248.
(13) Blossey, R.; Bosio, A. *Langmuir* **2002**, *18*, 2952.
(14) Bourges-Monnier, C.; Shanahan, M. E. R. *Langmuir* **1995**, *11*, 2820.
(15) Deegan, D.; Bakajin, O.; Dupont, T. F.; Huber, G.; Nagel, S. R.; Witten, T. A. *Nature* **1997**, *389*, 827.
(16) Deegan, D.; Bakajin, O.; Dupont, T. F.; Huber, G.; Nagel, S. R.; Witten, T. A. *Phys. Rev. E* **2000**, *62*, 757.
(17) Deegan, R. D. *Phys. Rev. E* **2000**, *61*, 475.
(18) Parisse, F.; Allain, C. *Langmuir* **1996**, *13*, 3598.
(19) Shanahan, M. E. R. *Langmuir* **1995**, *11*, 1041.
(20) Morris, S. J. S. *J. Fluid Mech.* **2001**, *432*, 1.
(21) Ehrard, P.; Davis, S. H. *J. Fluid Mech.* **1991**, *229*, 365.
(22) Hocking, L. M. *Phys. Fluids* **1995**, *7*, 2950.
(23) Cachile, M.; Benichou, O.; Poulard, C.; Cazabat, A. M. *Langmuir* **2002**, *18*, 8070.
(24) Clint, J. H.; Fletcher, P. D. I.; Todorov, I. T. *Phys. Chem. Phys.* **1999**, *1*, 5005.
(25) Epstein, P. S.; Plesset, M. S. *J. Chem. Phys.* **1950**, *18*, 1505.

10.1021/la7013946 CCC: $37.00
Published on Web 11/14/2007

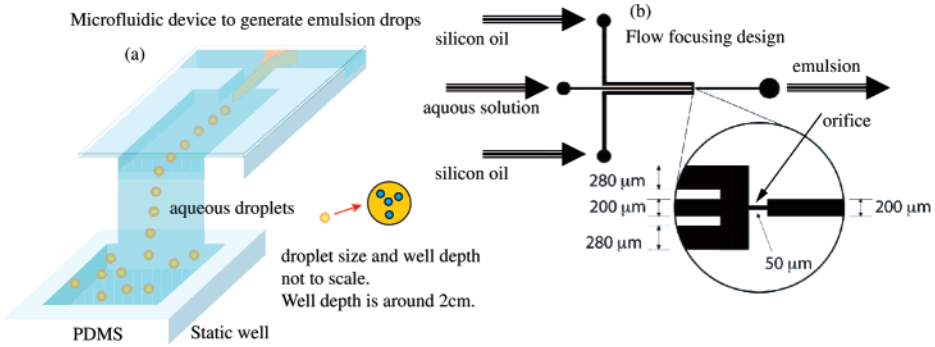

Figure 1. (a) Experimental setup: microfluidics device is used to produce micrometer-size aqueous droplets. Consequently, the droplets are collected in a static well for consolidation study. (b) Flow-focusing design to generate aqueous droplets in the oil phase.

by Duncan et al. for a gas−liquid system[26] and a liquid−liquid system (aniline−water system).[27] Frade and Cable[28] studied combined effects of diffusion and reaction on the growth or dissolution of spherical particles and showed that interface reaction could be important. More recently, Shedd[29] proposed a general model to estimate the dissolution time for bubbles that are stationary or moving within a fluid, with specific applications in immersion lithography. The dissolution processes described above all exhibit conventional diffusion-limited behavior, i.e., the mean squared diameter of a droplet decreases as a linear function of time. However, an increasing number of natural phenomena do not fit into this relatively simple description of diffusion. For example, deviation from Fickian-type diffusion has been observed in polymeric vesicle formations,[31] small particles moving in dense liquids,[32] and flow in heterogeneous porous media.[33]

The dissolution rate of the dispersed phase in an emulsion system can be expected to be strongly dependent on the dynamics of the consolidation process within emulsion droplets, which is the focus of this work. As a first step to understand how the consolidation process impacts the final colloidal packings, we investigate the temporal behavior of droplet shrinkage and the factors that affect this behavior. We study water-in-oil systems with silicone oil (SO) and fluorinated silicone oil (FSO) as the oil phases and examine the effects of initial droplet size, particle, and surfactant concentration.

2. Experiments

2.1. Experimental Setup. In this study, we use microfluidic devices to generate monodisperse aqueous droplets in an oil phase. As droplets travel in the microchannel at a high velocity (on the order of cm/s and higher) which makes it difficult to observe the consolidation, a static well is used to collect emulsion droplets exiting the microchannel (see Figure 1). Emulsion droplets are entrained in the static well before we conduct the consolidation study.

The microfluidic devices employed in this work are fabricated by soft lithography techniques.[34] First, polydimethylsiloxane (PDMS) is poured onto a silicon wafer mold patterned with a negative photoresist (SU-8, from MICROCHEM). Then, PDMS is cured in a convection oven at 60 °C for about 1 h and is bonded to a glass slide or a piece of PDMS to enclose the channel. By using a flow-focusing design,[35] the dispersed and continuous phases are both forced to pass through an orifice, causing the dispersed phase to taper to a tip with diameter smaller than that of the orifice (see Figure 1b). Subsequently, a tiny amount of fluid is broken off the tip to form a droplet. By adjusting the flow rates of the continuous and dispersed phases, droplet sizes can be controlled to range from 20 μm to several hundred micrometers in our experiments. By using microfluidic devices, we can easily adjust the droplet size and the number of particles entrapped in each droplet.

Table 1. Material Properties of Silicone Oil (SO) and Fluorinated Silicone Oil (FSO)

properties	SO	FSO
appearance and color	clear liquid	clear liquid
Solubility of Water in Oil	slightly soluble	slightly soluble
viscosity (Pa·s)	0.96	0.5
specific gravity	0.96	1.25
thermal conductivity (W/m·K)	0.159	0.028
specific heat (kJ/kg·K)	1.46	0.82

2.2. Materials. Silicone oil (PDMS) from Sigma and fluorinated silicone oil (polytrifluoropropylmethylsiloxane) FMS-123 from Gelest are shown by Yi et al.[9] to be PDMS compatible and slightly water soluble so are used here as the continuous phase in our water-in-oil system (see Table 1 for the material properties of the oil phases). Both SO and FSO have relatively high viscosity (400 and 1000 cSt, respectively) compared to that of water. Garstecki et al.[36] have shown that the volume of the bubbles formed in a flow-focusing channel decreases as the viscosity of the continuous liquid phase increases. By analogy, the viscosity ratio of continuous phase over dispersed phase is expected to be inversely related to droplet size. Thus, the use of the oil phase with higher viscosity tends to produce smaller droplets. Adding surfactants can reduce the interfacial energy, further decreasing the droplet size. The presence of surfactant can also prevent droplets from coalescing downstream in the channel. Among the several surfactants we have tried, Tween 20 (Aldrich) works very well in our system.

Colloidal particles (Polysciences, Inc.) are monodisperse latex beads with 2.0 μm mean diameter packaged as 2.5% aqueous suspension with coefficient of variance of 5%. The particles have a sulfate ester surface group that makes them hydrophobic, with average surface charge density of 4.8×10^{-2} C/m^2.

2.3. Consolidation Study with Static Setup. Due to the difficulty of microscopically observing droplets during both production and consolidation, we design a static setup containing a glass slide with a piece of PDMS bonded to it. Then, we punch a hole all the way through PDMS down to the glass slide to produce the well. The PDMS well can be used to collect the fluids coming out of the outlet channel (see Figure 2). The typical well depth is ~2 cm. Inside the well a thin layer of the continuous oil phase forms containing some water droplets. These experiments are performed under a controlled lab environment. The relative humidity is measured to be 60 ± 2% under a constant lab temperature of 70 °F.

For the two oil phases used in our experiments, FSO and SO are more and less dense than water, respectively. Water droplets therefore

(26) Duncan, P. B.; Needham, D. *Langmuir* **2004**, *20*, 2567.
(27) Duncan, P. B.; Needham, D. *Langmuir* **2006**, *22*, 4190.
(28) Frade, J. R.; Cable, M. *J. Mater. Sci.* **1995**, *30*, 989.
(29) Shedd, T. A. *J. Microlith. Microfab.* **2005**, *4*, 330041.
(30) Li, B.; Wang, J. *Phys. Rev. Lett.* **2003**, *91*, 044301.
(31) Battaglia, G.; Ryan, A. J. *J. Phys. Chem. B* **2006**, *110*, 10272.
(32) Bhattacharyya, S.; Bagchi, B. *J. Chem. Phys.* **1997**, *106*, 1757.
(33) Koch, D. L.; Brady, J. F. *Phys. Fluids* **1988**, *31*, 965.
(34) Xia, Y.; Whitesides, G. M. *Annu. Rev. Mater. Sci.* **1998**, *28*, 153.
(35) Anna, S. L.; Bontoux, N.; Stone, H. A. *Appl. Phys. Lett.* **2003**, *82*, 364.
(36) Garstecki, P.; Gitlin, I.; Diluzio, W.; Kumacheva, E.; Stone, H. A.; Whitesides, M. *Appl. Phys. Lett.* **2004**, *85*, 2649.

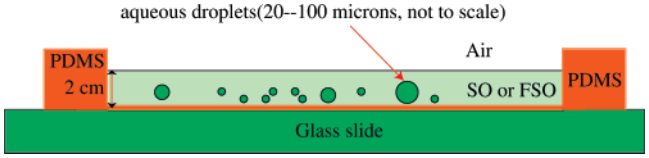

Figure 2. Well design for static study. Water is the dispersed phase. Note that the well depth is on the order of 200 times that of the droplet size; the schematics does not scale.

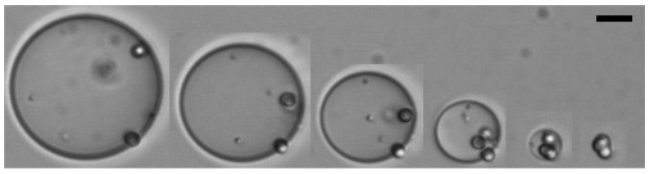

Figure 3. Sequence of frames of the consolidation process of a water droplet containing 3 PS beads (2 μm in diameter) in SO with viscosity of 1000 cSt. Scale bar is 10 μm. t_0 is defined as the net time duration between the start and the completion of the consolidation process, in this case, $t_0 = 140$ s.

rise in FSO and sink in SO. In our experiments, we find that droplets rising in FSO works well because droplets still remain below the FSO/air interface, i.e., they are always suspended entirely in the FSO without exposure to air. Furthermore, due to the high viscosity (1000 cSt) of the SO used in our experiments and the fact that its density is very close to that of water, the sinking velocity of aqueous droplets (e.g., droplets of diameter less than 100 μm) is small enough to allow the consolidation process to complete without disturbance. By using Stokes law, the droplet velocity in the static well is

$$V = \frac{2}{9}\frac{r^2 g(\rho_{fso} - \rho_w)}{\eta_{fso}} \text{ or } V = \frac{2}{9}\frac{r^2 g(\rho_w - \rho_{so})}{\eta_{so}} \qquad (2.1)$$

with r the droplet size, ρ_{fso} the density of FSO, ρ_{so} the density of SO, ρ_w the density of the aqueous droplet, η_{fso} the shear viscosity of FSO, and η_{so} the shear viscosity of SO. On the basis of the material properties provided in Table 1 and a droplet size on the order of 100 μm in diameter or less, the droplet velocity is estimated around 0.2 μm/s for droplet sinking in SO and around 3 μm/s for droplet rising in FSO. As the velocities for both cases are sufficiently small, convection can be neglected in the process. Furthermore, with the well depth being on the order of 2 cm, it will take the droplet more than 100 min to reach either the oil/air interface or the bottom of the well. The time scale for a droplet consolidation to complete is less than 800 s. With such disparity of time scale, we expect that the consolidation process should always be complete well before the droplets reach the bottom of the well of or the oil/air interface. Finally, we estimate the Peclet number to investigate whether flow associated with droplet rising/sinking influences the consolidation process. The Peclet number is defined by $\mathrm{Pe} = lV/D_{wo}$, with l the characteristic length scale (i.e., the droplet radius), V the droplet velocity, and D_{wo} the diffusivity of water in oil. For a typical droplet of radius 50 μm, the droplet rising velocity is on the order of 3 μm/s, and $D \approx 5 \times 10^{-6}$ cm^2/s (see Duncan and Needham[27]), $\mathrm{Pe} \approx 0.3$. This small value of the Peclet number indicates that flow effects are negligible.

3. Results and Discussion

3.1. Experimental Results. We study the dynamics of droplet shrinkage by taking a series of frames (Figure 3) as droplet size decreases with time. First, we examine the effect of the number of colloids inside a single droplet on the consolidation process. The dimensional plot is shown in Figure 4, in which d and t represent droplet diameter and time, respectively; the droplet size is fixed. The legend denotes the number of constituent particles in the droplet. We observe that the larger the number

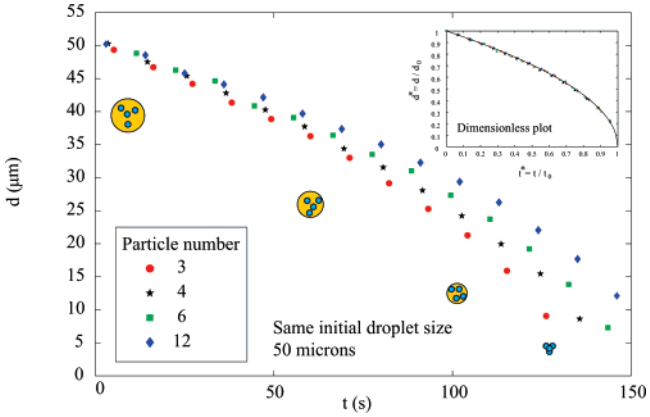

Figure 4. Effect of the number of constituent particles on the consolidation process of an aqueous droplet in silicone oil. The legend shows the number of constituent particles.

of constituent particles, the longer it takes for the consolidation process to complete. For example, a droplet with diameter 50 μm containing six particles shrinks faster than a droplet containing 12 particles given the same initial droplet size. Because the particles partition at the droplet interface (Figure 3), they hinder the removal progress of water into the surrounding oil phase. If a more significant portion of the droplet interface is occupied by the constituent particles, these particles could form a shell to prevent water from dissolving into the oil phase and could slow down the consolidation process, as we see at later times in Figure 4. This mechanism is physically different from that described by Subramaniam et al.[37] for the assembly of jammed colloidal shells on fluid droplets. The system used by Subramaniam et al. contains very high particle-number densities. When the number density is high and the particles are close packed, the mean curvature of the gas/water interface can change and induce a pressure jump that pushes water across the interface, forming colloidal shells on the droplet. In our study, due to our low particle concentration system, these curvature effects only become important at the late stage of the consolidation process. Furthermore, some recent studies[38−40] on the dynamics and collapse of 2D colloidosomes reported reduced colloidal diffusivity at the interface as the droplet radius decreases and approaches the colloidal size. Again, in our experiments, this effect is only likely to be important near the end of the consolidation process.

The non-dimensional plot of droplet size versus time is shown in Figure 5 in which the normalized time $t^* = t/t_0$ is plotted against the droplet diameter normalized by $d^* = d/d_0$, with d_0 the initial droplet diameter and the net time duration t_0 between the start and the completion of the consolidation process (see Figure 3). Note that water is never completely gone in the droplet at the end of the consolidation, in combination with the fact that t_0 is based on the microcopy images, t_0 is only an experimental estimate. All the experimental data fall on a single curve, which can be fit by a power-law relationship with an exponent of 1/2. As t_0 is obtained from experimental measurements (and therefore t_0 is not an intrinsic material property) that depend on the initial droplet size d_0 and particle number N, Figure 5 does reflect the effects of particle number N on the droplet consolidation process. More discussion on the interfacial area reduction due to particle number change during consolidation is presented in Section 3.2.

(37) Subramaniam, A. B.; Abkarian, M.; Stone, H. A. *Nat. Mater.* **2005**, *4*, 553.
(38) Einert, T.; Lipowsky, P;, Schilling, J.; Bowick, M. J.; Bausch, A. R. *Langmuir* **2005**, *21*, 12076.
(39) Tarimala, S.; Wu, C.; Dai, L. L. *Langmuir* **2006**, *22*, 7458.
(40) Wang, C.; Liu, H.; Gao, Q.; Liu, X.; Tong, Z. *Chem. Phys. Chem.* **2007**, *8*, 1157.

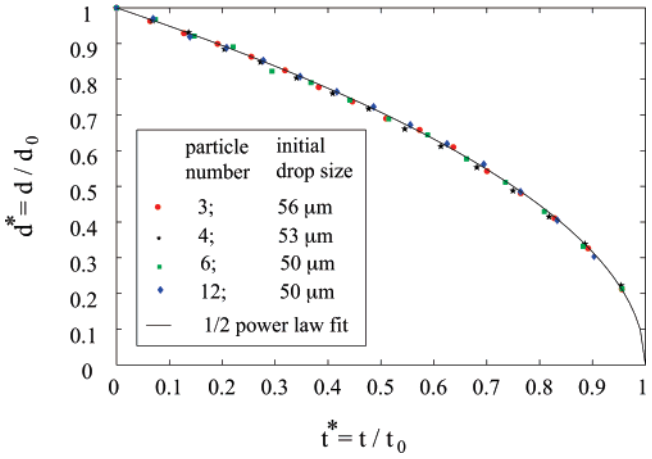

Figure 5. Normalized plot of consolidation process for aqueous droplets with different number of constituent particles in silicone oil. t_0 is measured experimentally and reflects the droplet size and particle number effects implicitly.

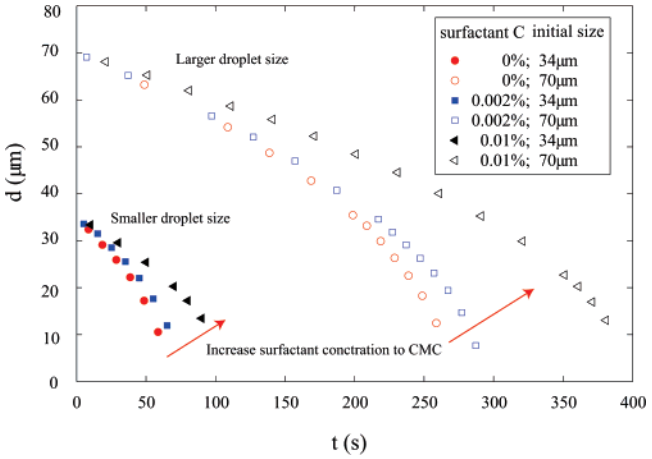

Figure 6. Effect of surfactant concentration and initial droplet size on the consolidation process of water droplet in silicone oil. The legend indicates surfactant concentration. The critical micelle concentration of Tween20 is 0.007% by weight.

The effect of surfactant on the consolidation process is shown in Figure 6. Water-soluble surfactant Tween 20 (CMC 0.007% w/w) with three different concentrations was used in the dispersed phase for comparison, and the concentration values are indicated in the legend. For small surfactant concentration values (0.002%, c < CMC), droplets with similar sizes take approximately the same time to shrink down as in the case of no surfactant added at all, indicating that the effect of surfactant concentration on the consolidation process is negligible as long as the surfactant concentration stays low compared to its CMC value. For highly concentrated surfactant aqueous solution, however, the consolidation process slows down significantly, as shown in Figure 6. In the case of surfactant concentration of 0.01%, it takes at least 30% longer to remove all the water in the droplet compared to droplets with surfactant concentration 0.002% or lower.

Normalized the same way as in Figure 5, all the data collapse on a single curve (shown in Figure 7), suggesting that although surfactant can facilitate emulsification, function as a stabilizer, and have impact on the consolidation time of water droplets, it does not change the power law behavior of the consolidation process. Moreover, Figure 7 shows all data (varying surfactant concentration, initial droplet size, and number of constituent particles) in the same figure, and they fall on a single curve, further confirming that the droplet shrinkage process is governed

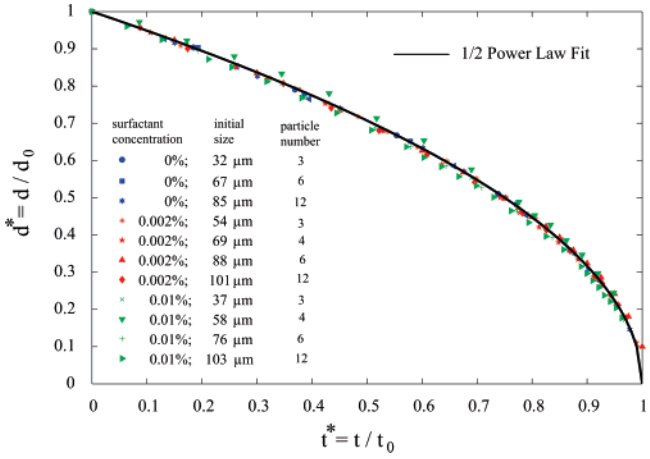

Figure 7. Normalized plot of consolidation process of aqueous droplets in silicone oil for different surfactant concentrations, initial droplet size, and particle numbers.

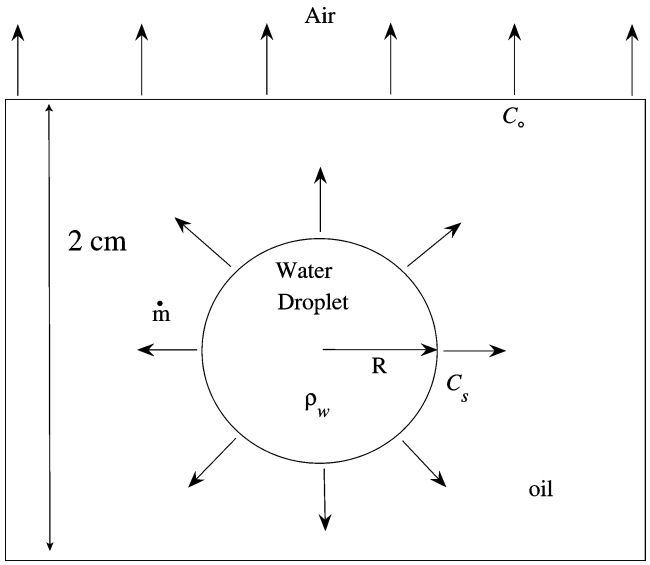

Figure 8. Schematic illustrating a shrinking droplet. The droplet size is on the order of 50−100 μm in diameter (not to scale in figure).

by the same power law with the proper scaling. Here, t_0 is an experimental measured quantity that reflects the effects of the number of the constituent particles, surfactant concentration, or initial droplet sizes.

3.2. Diffusion Controlled Model. When the consolidation process occurs, four mechanisms take place simultaneously (Figure 8): water diffuses into the oil phase, water dissolves into the oil phase through the droplet/oil interface, water crosses the emulsion/air interface, and vapor convects to infinity. Among these mechanisms, vapor convection is the fastest. Since the experiments reported above show that the droplet radius varies at square root of time with varying experimental conditions, we assume that diffusion of water molecules in the oil phase is the rate-controlling mechanism at isothermal conditions. Based on the Epstein−Plesset model[25] that captures the diffusion-limited process, neglecting the convection term, the concentration of the droplet follows

$$\frac{\partial c}{\partial t} = D_{wo}\left(\frac{\partial^2 c}{\partial r^2} + \frac{2}{r}\frac{\partial c}{\partial r}\right) \tag{3.1}$$

with c the concentration of the aqueous phase, D_{wo} the diffusivity coefficient of the aqueous phase in the oil phase. We assume that the concentration of dissolved water is uniform and equal to c_0 and the concentration of water at the droplet surface is a constant, c_s. Hence, the boundary conditions can be imposed as

$$c(r, 0) = c_0,\ r > R;\ c(R, t) = c_s,\ t > 0;\ c(r, t) = c_0 \text{ when } r \to \infty \quad (3.2)$$

Solving eq 3.1 with the boundary conditions in eq 3.2, we obtain the concentration gradient at the droplet interface:

$$\frac{\partial c}{\partial r} = (c_0 - c_s)\left(\frac{1}{R} + \frac{1}{\sqrt{\pi D_{wo} t}}\right) \text{ at } r = R \quad (3.3)$$

The mass flux of water across the interface is

$$\frac{dm}{dt} = 4\pi D_{wo}\rho_w R^2\left(\frac{\partial c}{\partial r}\right)_{r=R} \quad (3.4)$$

This relationship is only valid for a stationary droplet interface. We will use this approximation for a droplet with moving boundary. Hence,

$$4\rho_w \pi R^2 \frac{dR}{dt} = 4\pi\rho_w D_{wo} R^2\left(\frac{\partial c}{\partial r}\right)_{r=R} \quad (3.5)$$

If the diffusion of water molecules in the oil phase is rate-limiting, we assume that the density of water, ρ_w, is constant inside the droplet, the droplet radius obeys

$$\frac{dR}{dt} = D_{wo}(c_0 - c_s)\left(\frac{1}{R} + \frac{1}{\sqrt{\pi D_{wo} t}}\right) = \frac{D_{wo}(c_0 - c_s)}{R}\left(1 + \frac{R}{\sqrt{\pi D_{wo} t}}\right) \quad (3.6)$$

The first and second terms on the right-hand side of eq 3.6 encompass steady state and transient effects, respectively. For a typical droplet size of radius 50 μm, the time required to complete the consolidation is on the order of 150 s, with an estimated diffusivity constant $D_{wo} \approx 5 \times 10^{-6}$ cm^2/s and the steady-state term is about an order of magnitude greater than the transient term. The steady-state term therefore dominates in our experimental system. If, consistent with this, we neglect the transient term, using the boundary conditions $r = 0$ at $t = t_0$ and $r = R_0$ at $t = 0$, with R_0 the initial droplet radius and t_0 the consolidation time, we obtain

$$R = R_0[2D_{wo}(c_s - c_0)]^{1/2}(t_0 - t)^{1/2} \quad (3.7)$$

The solution, eq 3.7, illustrates that droplet radius R (or the diameter d) scales with time t as $(t_0 - t)^{1/2}$, which is in good agreement with our experimental data, indicating that consolidation is diffusion-controlled and the assumptions of constant D_{wo}, c_0, and c_s is reasonable in our case. Furthermore, if we keep the transient term in eq 3.6, the solution yields more complicated structures[25] but the droplet size R still changes with respect to $t^{1/2}$.

We also investigate whether the scalings obtained from our experimental measurements are consistent with the diffusion model proposed above. We nondimensionlize eq 3.6 and introduce the characteristic length scale R_0 (droplet initial radius), particle number N, and characteristic time scale t_0 (the net duration time for the consolidation process) to account for the particle number and droplet initial size effects. The dimensionless variables are denoted with a star as follows. $R^* = R/NR_0$, $t^* = t/t_0$. The dimensionless form of eq 3.6 then reads

$$\frac{dR^*}{dt^*} = D_{wo}(c_0 - c_s)\left(\frac{\alpha}{R^*} + \sqrt{\frac{\alpha}{\pi D_{wo} t^*}}\right), \text{ with } \alpha = \frac{t_0}{(R_0 N)^2} \quad (3.8)$$

To obtain the power law scaling as observed from experiments, $R^* \propto t^{*1/2}$, α must be a constant. We plot t_0 vs R_0N from our experimental data and show that $t_0 \propto (R_0N)^2$, i.e., α is approximately a constant based on our experimental data. Figure 9 verifies that diffusion controlled model is a good estimate to capture the consolidation process observed in our experiments.

Finally, we emphasize that the diffusion controlled model discussed above does not account for the loss of spherical symmetry during consolidation; further studies designed to probe this phenomenon should be conducted in the future.

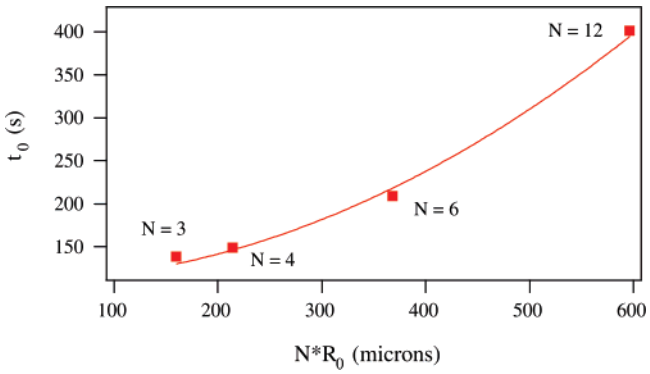

Figure 9. Consolidation time t_0 is plotted against NR_0 with different initial droplet size and particle numbers. The solid line is a power law fitting with 2.0 exponent.

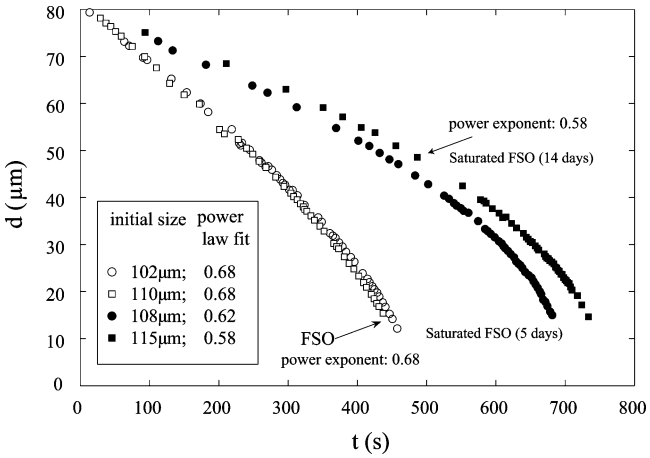

Figure 10. Dimensional plot of consolidation process for water/FSO system (open symbols) and water/FSO saturated system (closed symbols). The first column in the legend denotes the initial droplet sizes. The second column is the power exponent for the curve fit of the consolidation process.

4. Deviation from the Conventional Diffusion Model

When we replace SO with FSO as the continuous oil phase, the exponent increases from 1/2 to 2/3, as shown in Figure 11 by the closed symbols. Typically, in a diffusion process, the mean squared displacement of a particle (or droplet radius) is a linear function of time, i.e., $d \sim t^{1/2}$, also known as conventional-

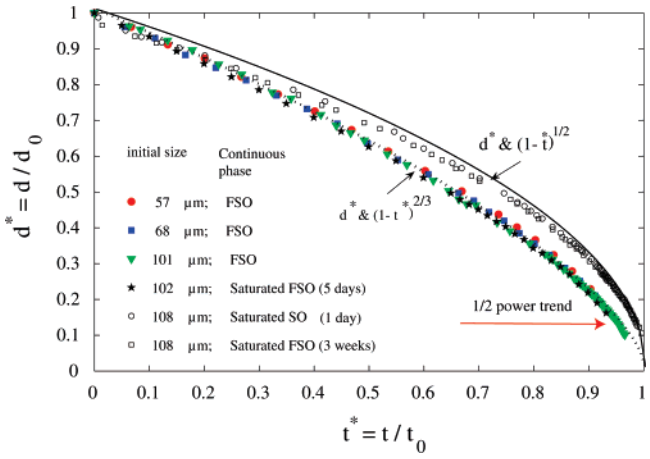

Figure 11. Normalized plot of consolidation process for a different oil phase (FSO).

type diffusion. Hansen[41] recently reviewed the aspects of solubility, surfaces, and diffusion in polymers and pointed out that the balance between the concentration-dependent diffusion resistance and the surface resistance would determine whether the diffusion is Fickian-type.

To investigate the deviation of conventional diffusion behavior of droplet consolidation in FSO, we first probe whether D_{wo} is a function of the water concentration. To examine this speculation, we mix water and FSO thoroughly (90% water by weight), and let the mixture sit for at least 1 week to ensure sufficient saturation. We then use this saturated FSO as the continuous oil phase to absorb water from droplets for consolidation studies. The power exponent for saturated FSO of 5 days is 0.62, while the power exponent for saturated FSO of 2 weeks is 0.58 (see Figure 10). Both exponents lie between 1/2 and 2/3, suggesting that diffusivity D_{wo} depends on the water concentration and the saturation level of the oil phase. We further conduct experiment with saturated SO (saturation time varying from 2 to 14 days) as the continuous oil phase and observe the same exponent 1/2, indicating that D_{wo} of SO is independent of water concentration. Our experimental observation suggests that a steady-state approximation of the diffusion model becomes more valid as the dissolution lifetime increases relative to the time required for the stationary layer formation at the oil−water interface. Indeed, if we choose the ending portion of a consolidation process for FSO where the droplet size becomes close to zero, the exponent changes toward 1/2. This observation also provides us a way of comparing the magnitude of the diffusivity of one liquid (e.g., water) in two oil phases (e.g., FSO and SO). Keeping the other experimental conditions the same, the oil in which consolidation shows a higher exponent should have smaller diffusivity. Furthermore, we notice that the dissolution time increases with the increasing saturation level, which is consistent with the recent study of microdroplet dissolution of aniline−water system by Duncan and Needham.[27]

Since the atmosphere outside the oil affects transport during the consolidation process, the relative humidity of the air can be adjusted to change the saturation level of the oil/water system. In our experiment, all experiments are performed in a controlled lab environment with the air relative humidity 60 ± 2%. Future studies can be conducted by creating an environmental chamber to vary the relative humidity level.

Another possible factor contributing the deviation of conventional diffusion behavior for the FSO case is the interfacial effects between the oil and aqueous phases. Tween 20 might produce a viscoelastic monolayer at the interface between water and oil,[42] and the nature of the viscoelasticity will depend on the oil used. Further studies need to be conducted.

5. Conclusions

The dynamics of water removal from the droplet into the oil phase, i.e., the consolidation process, is studied in this work. The effects of the number of particles inside the droplet and the surfactant concentration of the aqueous solution are investigated. The existence of particles at the droplet interface tends to slow down the consolidation process, but the effect is negligible as long as the number of inside particles stays low. Surfactant slows down the consolidation process. With proper scalings, the consolidation process obeys the same power law for a specific continuous oil phase, irrespective of the change in the number of constituent particles and the surfactant concentration. The power exponent for the consolidation process varies for different oil phases. With SO (and saturated) being the continuous phase, Fickian (concentration independent)-type diffusion is observed. With un-saturated and saturated fluorinated silicone oil being the continuous phase, a deviation from conventional diffusion is observed. Experimental observations indicate that this deviation can be attributed to the concentration and interfacial effects during the consolidation process. Our study establishes a systematic characterization of microstructure evolution at liquid−liquid interfaces during consolidation that has fundamental importance for protein crystallization, drug delivery, and nanometer-scale material synthesis.

Acknowledgment. We gratefully acknowledge support from National Science Foundation CBET CAREER award-57800. We also thank referees for many helpful comments. Finally, we thank Professor Eliot Fried and Xuemei Chen for useful discussions.

LA7013946

(41) Hansen, C. M. *Prog. Org. Coat.* **2004**, *51*, 55.

(42) Dickinson, E. *Soft Matter* **2006**, *2*, 642.